J Neurophysiol 89: 2961–2974, 2003.
First published February 5, 2003; 10.1152/jn.01065.2002.

Electrical Stimulation of the Supplementary Eye Fields in the Head-Free Macaque Evokes Kinematically Normal Gaze Shifts

Julio C. Martinez-Trujillo, Hongying Wang, and J. Douglas Crawford
Centre for Vision Research and Canadian Institute for Health Research, Group for Action and Perception, Departments of Psychology, Biology and Kinesiology and Health Sciences, York University, Toronto, Ontario M3J 1P3, Canada

Submitted 26 November 2002; accepted in final form 31 January 2003

Martinez-Trujillo, Julio C., Hongying Wang, and J. Douglas Crawford. Electrical stimulation of the supplementary eye fields in the head-free macaque evokes kinematically normal gaze shifts. *J Neurophysiol* 89: 2961–2974, 2003. First published February 5, 2003; 10.1152/jn.01065.2002. The supplementary eye fields (SEFs), located on the dorsomedial surface of the frontal cortex, are involved in high-level aspects of saccade generation. Some reports suggest that the same area could also be involved in the generation of motor commands for the head. If so, it is important to establish whether this structure encodes eye and head commands separately or gaze commands that give rise to coordinated eye-head movements. Here we systematically stimulated (50 μA, 300 Hz, 200 ms) the SEF of two head-free (head unrestrained) macaques while recording three-dimensional eye and head rotations. A total of 55 sites were found to consistently elicit saccade-like gaze movements, always in the contralateral direction with variable vertical components, and ranging in average amplitude from 5 to 60°. These movements were always a combination of eye-in-head saccades and head-in-space movements. We then performed a comparison between these movements and natural gaze shifts. The kinematics of the elicited movements (i.e., their temporal structure, their velocity-amplitude relationships, and the relative contributions of the eye and the head as a function of movement amplitude) were indistinguishable from those of natural gaze shifts. Additionally, they obeyed the same three-dimensional constraints as natural gaze shifts (i.e., eye-in-head movements obeyed Listing's law, whereas head- and eye-in-space movements obeyed Donders' law). In summary, gaze movements evoked by stimulating the SEF were indistinguishable from natural coordinated eye-head gaze shifts. Based on this we conclude that the SEF explicitly encodes gaze and that the kinematics aspects of eye-head coordination are implicitly specified by mechanisms downstream from the SEF.

INTRODUCTION

A number of recent reports have elaborated on the role of the dorsomedial frontal cortex in the cognitive aspects of gaze control (Bon and Lucchetti 1992, 1997; Chen and Wise 1995a,b; Coe et al. 2002; Lu et al. 2002; Olson and Gettner 1999; Olson and Tremblay 2000; Schall 1991; Schiller and Tehovnik 2001; Schlag 2002), but the nature of the motor command generated by this area remains unclear. Early physiological studies in nonhuman primates reported that electrical stimulation of the dorsomedial surface of the frontal lobe elicited head movements (Levinsohn et al. 1909). Later studies employed more advanced techniques to measure head and eye movements and reported that predominantly eye-in-head saccades were elicited when stimulating an area within the same dorsomedial surface of the frontal lobe in macaques (Schlag and Schlag-Rey 1987). These and subsequent authors have defined this area as the supplementary eye field (SEF) (Bon and Lucchetti 1992; Fujii et al. 1995; Missal and Heinen 2001; Mitz and Godschalk 1989; Russo and Bruce 1993, 1996, 2000; Tehovnik et al. 1994, 1998, 1999). Recent preliminary reports have suggested that the SEF could encode combined movements of both the eyes and the head (Chen and Sparks 2001; Martinez-Trujillo et al. 2002). The goal of the present study is to determine whether most sites in the SEF encode just eye commands, separate eye and head commands, or gaze commands giving rise to coordinated eye-head movements.

One way of addressing this question is by examining eye and head rotations resulting from stimulating the SEF in head-free monkeys. However, the majority of the stimulation studies in this area have been conducted in head-fixed animals (Bon and Lucchetti 1992; Mitz and Godschalk 1989; Russo and Bruce 1993; Tehovnik et al. 1994, 1998). Head-free stimulation of other structures, such as the superior colliculus (SC), have resulted in combined movements of the eye and the head (Freedman et al. 1996; Guillaume and Pelisson 2001a,b; Klier et al. 2001; Pelisson et al. 1989; Roucoux et al. 1980). These movements were kinematically indistinguishable from natural gaze shifts, suggesting that the SC encodes gaze. In addition, head-free stimulation of the frontal eye field (FEF) evokes combined movements of the eye and the head that appear qualitatively similar to natural gaze shifts (Tu and Keating 2000). Based on this, it seems likely that higher level structures like the SEF also encode gaze. However, to answer this question, a detailed quantitative analysis comparing the kinematics of stimulation-evoked movements and natural gaze shifts must be performed.

The experimental goals of this study were to see if the SEF stimulation evokes both eye and head movements and, if so, to determine whether these movements obey the same kinematics rules as natural gaze shifts. If they do obey the same kinematics rules, it would suggest that the motor output of the SEF is gaze. An opposite result would suggest that the SEF is involved in the generation of separate commands for the eyes and the head. We chose three criteria that have been used in similar inves-

Address for reprint requests: J. Cesar Martinez-Trujillo, Dept. of Psychology, 209 Behavioural Sciences Bldg., York University, 4700 Keele St., Toronto, Ontario, M3J 1P3, Canada (E-mail: trujillo@yorku.ca).

The costs of publication of this article were defrayed in part by the payment of page charges. The article must therefore be hereby marked "*advertisement*" in accordance with 18 U.S.C. Section 1734 solely to indicate this fact.

tigations of gaze coding in head-free monkeys to compare the kinematics of stimulation-evoked movements and natural gaze shifts (Freedman et al. 1996; Guillaume and Pelisson 2001a,b; Klier et al. 2001). These criteria summarize a set of kinematics rules obeyed during natural gaze shifts in the head-free monkey. The first two have been used by Freedman et al. (1996) to determine if the motor output of the SC encodes gaze as described further here.

First, the amplitude-velocity relationship or main sequence: during natural gaze shifts the gaze, head, and eye movements peak velocities vary stereotypically as a function of movements amplitude (Freedman and Sparks 1997; Freedman et al. 1996). While gaze and eye peak velocities are saturated functions of gaze amplitude, head peak velocity increases approximately linearly with gaze amplitude. Second, relative contributions of the eyes and the head movements to gaze amplitude: during natural gaze shifts, the head movements contribution seems to be almost negligible for gaze amplitudes smaller than 20°. For gaze amplitudes larger than 20°, such a contribution increases linearly with the amplitude of the movement. On the other hand, the contribution of the eyes to gaze starts for the smallest gaze amplitudes, and grows linearly with the amplitude of the movement until reaching saturation for movements larger than 35° (Freedman et al. 1996; Freedman and Sparks 1997; Tomlinson and Bahra 1986). Freedman et al. (1996) found that both of these relationships held in gaze shifts evoked by SC stimulation. Based on this and other criteria, they concluded that the SC encodes gaze. Thus if the SEF also outputs a gaze command to the motor systems, one would expect the same rules to hold in movements evoked by SEF stimulation.

The third criterion refers to Donders' law of eye and head. It is known that for every possible two-dimensional gaze direction, the eyes possess a fixed amount of torsion about a nasal-occipital axis (Donders 1848). When the head is fixed, a special form of Donders' law, Listing's law, is obeyed (Ferman et al. 1987a,b; Helmholtz 1867; Tweed and Vilis 1990). Listing's law states that when the head is fixed, the eyes assume only those orientations that can be reached from a central reference position by rotation about axes that lie in a plane. As a consequence, the torsional angle of the eyes relative to that plane is always zero.

During fixations between natural head-free gaze shifts in human subjects (Glenn and Vilis 1992; Radau et al. 1994) and monkeys (Crawford and Vilis 1991; Crawford et al. 1999), similar laws are obeyed. The head seems to follow a form of Donders' law called the Fick strategy, and the eyes-in-head seems to follow Listing's law. However, to achieve the latter, a precise eye-head coordination is necessary because many times the brain must predict the amount of torsion produced by the vestibuloocular reflex (VOR) during the final "slow phase" of the movement (Crawford and Vilis 1991; Crawford et al. 1999; Tweed 1997).

Klier et al. (2001) have stimulated the SC and found that the resultant gaze shifts obeyed the same three-dimensional constraints. This is not trivial, because eye and head movements that are not associated with gaze shifts do not obey these constraints (Ceylan et al. 2000). Likewise, stimulation of some brain stem areas result in large torsional violations of Donders' law of the eyes and head (Crawford et al. 1991; Klier et al. 2002a). Although Klier et al. (2002b) concluded that Donders' law was implemented downstream from the SC, it is known that humans can voluntarily violate Donders' law of the eyes and head (Ceylan et al. 2000), suggesting that there is a cortical override mechanism. Therefore a three-dimensional analysis of stimulation-evoked movements provides another diagnostic test to determine if the SEF encodes natural gaze shifts or other motor aspects of eye-head coordination.

We hypothesized that if the SEF encodes gaze, electrical stimulation of most sites in this area would elicit combined movements of the eyes and the head that follow the same kinematics laws as natural gaze shifts. We found that SEF stimulation elicited combined movements of the eyes and the head. These movements were indistinguishable in their velocity-amplitude profiles, their relative eyes and head contributions as a function of gaze amplitude, and three-dimensional constraints (Donders' and Listing's law) from natural gaze shifts. Our results suggests that the SEF encodes gaze and that the details of eye-head coordination during natural gaze shifts are specified downstream from this area.

METHODS

Preparation of the animals

Two monkeys (*Maccaca mulatta*) were surgically prepared for three-dimensional (3-D) eye- and head-movement recordings. Each animal underwent a general anesthesia, during which 3-D homemade coils (copper wired covered by silicone) were implanted on the right eye. An acrylic cap was attached to the animals' skull through orthopedic screws, and a metal head post was embedded on the acrylic. A small plastic piece was also embedded on the acrylic to give support to two perpendicularly oriented coils, similar to the ones implanted in the eyes, used during the recordings to measure the head orientation. Finally, a recording chamber (20 mm diam) was positioned on the frontal bone with its center located at 25 mm anterior and 0 mm lateral in stereotaxic coordinates. A craniotomy of the frontal bone (20 mm diameter) covered the base of the chamber, allowing access to the left and the right SEFs. All these procedures were in accordance with the Canadian Council on Animal Care guidelines and were preapproved by the York University Animal Care Committee.

Experimental setup

Each monkey wore a primate jacket and sat in a modified Crist Instruments primate chair such that its head and neck were free to move as desired. The upper body (to the shoulders) was prevented from rotating in the yaw direction (i.e., movement around an earth-vertical axis) by the use of plastic molding and restraints that attached the primate jacket to the chair. The head of the animal was positioned in the middle of three mutually perpendicular magnetic fields (90, 125, 250 kHz). In each trial, animals looked toward a fixation light-emitting diode (LED) that was randomly chosen among nine different LEDs arranged in a 3×3 square array in which nearby elements were separated by 40° and rows and columns were parallel to the horizontal and vertical meridians, respectively. The LED positioned at the center of the array was aligned with the straight-ahead gaze-pointing direction and was used at the beginning of the experimental sessions to determine the reference position used for computing position quaternions from the coil signals (see following text). Coil signals were recorded using a sampling frequency of 100 Hz in *animal M1* and a frequency of 1000 Hz in *animal M2*.

Training and gaze control

Animals were trained (head-free) to direct their gaze toward the spatial location where an LED was previously flashed for an interval of 500 ms. If gaze was maintained at that location within a fixation window that ranged in diameter from 5 to 10° for a period of 2000 ms, a reward (drop of juice) was provided to the animal. Otherwise, animals were not rewarded and a "punishment" pause of ≥5000 ms was introduced before the next fixation target appeared. Each training session lasted for ~30 min. Animals were trained in this fixation task until they performed correctly in ≥80% of the trials, whereupon we began the experiments. During experimental sessions, performance was not systematically evaluated because in a substantial proportion of the trials fixation was artificially broken by the stimulation procedure. However, experiments were interrupted if the animals failed to keep maintain fixation in a substantial proportion of the trials where the stimulation was not delivered. During the training and recording sessions, head movement was not constrained except at the beginning and end of the sessions when the coil connectors, microdrive, and electrode had to be positioned or removed from their correspondent positions. We intentionally minimized the time when the animals had their head restrained to avoid the development of unnatural eye-head coordination strategies.

Unlike some stimulation studies (Chen and Sparks 2001; Sparks et al. 2001), our animals were not systematically trained to dissociate the relative pointing directions of the eyes and the head (i.e., gaze pointing to the right and head pointing to the left of the vertical meridian) when delivering the stimulation. They were free to choose the combination of eye-head positions when fixating the targets. Again, this was done to avoid contaminating the natural eye-head coordination patterns and to elicit these eye/head movements from natural combinations of eye/head position. In such cases, the eye and head are roughly aligned toward the target but depart from perfect alignment as a function of gaze direction and other factors (Freedman et al. 1996; Gandhi and Sparks 2001).

Stimulation

During each experimental session, one or several electrode penetrations were made using a mechanical microdrive (Narishigi model MO-99S) positioned on the top of a recording chamber and Platinum-Iridium glass covered microelectrodes (FHC) with impedances ranging from 0.5 to 3MΩ. In both animals, the penetrations covered a substantial portion of the recording chamber area on both sides of the midline. The electrode was advanced until the action potentials of single neurons were isolated on an oscilloscope. Subsequently, animals engaged in the trained fixation task and microstimulation trains were delivered at a random time within the 2000-ms fixation period after the LED flash when no visual stimulus was present. This procedure has been proved to elicit movements at low stimulation thresholds (Tehovnik et al. 1999). Stimulation trials did not exceed >50% of the total number of fixation trials, and both kinds of trials were intermixed. If eye-in-space (Es) movements were consistently evoked by delivering few stimulation trains (10–20 trains with intensities of 50 μA; duration, 200 ms; frequency, 300 Hz), we proceeded to test the correspondent site by delivering a number of stimulation trials (~50), separated by time intervals of ≥3000 ms. The stimulation parameters were chosen in the following way. First, we set the frequency (300 Hz), single pulse duration (0.2 ms), and train duration (200 ms) similar to the ones used in previous studies in the SEF (Schlag and Schlag-Rey 1987) and also in the SC (Freedman and Sparks 1996; Klier et al. 2001) where stimulation with similar parameters has proved to consistently evoke gaze shifts composed of head-in-space (Hs) and eye-in-head (Eh) movements. Second, we determined, for each site, the current intensity threshold for evoking gaze shifts. For all the sites included in the analysis, such thresholds were between 30 and 50 μA. Then the stimulation intensity was set slightly above thresholds (50 μA). Observe that these intensity threshold values are very similar to the ones reported by the original study of Schlag and Schlag-Rey (1987) in the SEF for evoking eye movements. An additional criterion that has already been proposed for the SC stimulation was taken into account to choose the stimulation parameters. The train duration (200 ms) was higher than the sum of the movements latencies and gaze shifts duration (Freedman et al. 1996).

By stimulating the SEF, a total of 82 sites (67 in *M1* and 15 in *M2*), where Es movements were systematically evoked, were isolated. These sites were located within an area between 23–30 mm anterior and 3–7 mm lateral in stereotaxic coordinates on both sides of the midline. The surrounding regions were also thoroughly explored, but stimulation of these areas did not evoke any noticeable Es or Hs movement under the stimulus and behavioral conditions of our experiment.

Data analysis

From the raw coil signals we computed quaternions to represent the orientation of the Es and Hs with respect to the reference position (Tweed et al. 1990). The quaternions were expressed in a right-hand coordinate system aligned with the coils. The orientation of the Eh were computed by inverting the Es quaternions and multiplying them by the correspondent Hs quaternions (Glenn and Vilis 1992). All the quaternions (Es, Hs, and Eh) were converted into 3-D vectors scaled by their angle of rotation (Crawford and Guitton 1997) as well as into angular velocity vectors for the off-line analysis. From the position quaternions, 2-D gaze trajectories were also obtained (Tweed et al. 1990). For the Es, these trajectories describe changes in the line of sight as if one were observing the animal from behind and its fovea were projecting a spot of light onto a hemisphere centered on the eye (see Fig. 8).

Angular Es, Hs, and Eh velocities were calculated for each stimulation-evoked movement. These were then averaged across all the movements for a given site and plotted as a function of time from the stimulation onset. A given site was accepted for further analysis only when a clear Es global velocity profile with an increase occurring during the 200-ms stimulation period, followed by a peak that reached ≥100°/s and finally a decrease to the initial levels was identified. Sites with flat Es velocity profiles in which this sequence was not identified were discarded. In such sites, the movements had variable latencies and either were not caused by the stimulation or the procedure gave unstable results. From the 82 sites, 55 sites met the inclusion criteria (45 in *M1* and 10 in *M2*).

For the included sites, the quaternions were plotted as a function of time and those representing eye positions at the beginning and end of each stimulation-evoked gaze shift were manually selected by an observer. A set of natural gaze shifts were selected during each recording sessions to be used as a control for the stimulation data. These natural movements were intermixed with the stimulation trials and were selected in such a way that for every Es initial and final position of the stimulation-evoked movements, there was at least one comparable natural movement with a similar Es initial and final position. After this procedure, we made sure that the two movement samples were similar and therefore their movements' kinematics could be reasonably compared. The 3-D position vectors from the stimulus-evoked selected signals were used to compute the amplitude of each gaze shift as well as the characteristic vector (CV) for Es, Hs and Eh at each site. Such a CV was computed through a multiple linear regression procedure performed on the stimulus induced movement displacement as a function of initial position (Klier et al. 2001). It describes the theoretical gaze trajectory that would be elicited if the eyes and head were initially pointed straight ahead. This method has the advantage of being robust to variations in the spatial distribution of initial eye positions.

The comparisons between the main sequences and relative contributions of the eyes and the head to the movements of the stimulation

evoked movements and natural gaze shifts was made using a one-way ANOVA test with gaze shift type as a within-subject factor.

3-D analysis

To determine how well the stimulation-evoked movements follow the 3-D constraints described for natural gaze shifts in the monkey (i.e., Listing's law), we quantified the 3-D range of orientations for the Es, Hs, and Eh: first during periods of normal fixations (Es and Hs velocities $<10°/s$) and second at the end of the stimulation-evoked head movements. This velocity threshold of 10°/s has been used in previous 3-D studies of macaques (Crawford et al. 1999), and it is an operational definition for the purposes of the study. This was done by determining the three surfaces (Es, Hs, and Eh) that are second-order surfaces of best fits to the correspondent position quaternions (Crawford et al. 1999; Glenn and Vilis 1992; Medendorp et al. 1998; Misslisch et al. 1998; Radau et al. 1994; Theeuven et al. 1993; Tweed and Vilis 1990; Tweed et al. 1990). The second-order surface is described by the equation $q_1 = a_1 + a_2q_2 + a_3q_3 + a_4(q_2)^2 + a_5q_2q_3 + a_6(q_3)^2$, which expresses torsional position (q_1) as a function of vertical (q_2) and horizontal (q_3) position. This equation is an analogue of a linear regression model in a two-dimensional space. For both data sets (fixation points and end of stimulation-evoked head movements), we computed the torsional variability or torsional SDs. This measurement indicates how closely the orientations of Es, Hs and Eh cluster around their surfaces. The smaller the torsional SD, the closer the quaternions adhere to their surface (Crawford et al. 1999; Tweed et al. 1990).

Anatomical reconstruction of the recording sites

After the experiments, the two animals were killed and anatomical reconstructions of the stimulation sites were made. For this purpose, the position of the recording chamber borders relative to the brain surface was determined and high-resolution digital images of the entire brain from different views were taken. The reconstruction of the penetration sites was made by superimposing a digital grid onto the chamber location. The *x* and *y* coordinates of each penetration site were prelocated within the grid and then re-mapped onto the brain surface (Fig. 1, ●). All the stimulation sites where eye and head movement were systematically evoked were located anterior to the genu of the arcuate sulcus at both sides of the midline within the region reported by other authors as the SEF in the macaque (see Tremblay et al. 2002). The data and conclusions in the following sections only applies to the sites of the dorsomedial frontal cortex indicated in Fig. 1.

RESULTS

After a thorough exploration of the recording chambers, we identified (on-line) 82 SEF sites in the two animals (67 in *M1* and 15 in *M2*) where stimulation evoked gaze shifts. In an off-line analysis, we found that in 55 sites (45 in *M1* and 10 in *M2*), we consistently evoked Hs and Eh movements with regular latencies (see METHODS). The subsequent sections present our analysis of these 55 sites. The first column in Fig. 2 shows two examples of the horizontal components of these movements (ordinate) as a function of time from stimulation onset (abscissa) from two different SEF sites in *animal M1*. The solid thin lines represent Es, the solid thick lines Hs, and the dashed lines Eh. In both cases, we can identify two main phases of the movement. The first (gaze shift phase) starts when Es starts moving (Hs and Eh also move during this phase) and finish when Es become stationary. The second

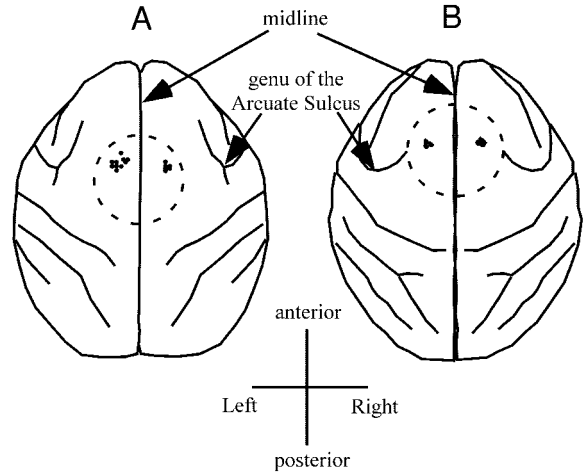

FIG. 1. Anatomical reconstruction of stimulation sites. Top view of the anatomical reconstruction of the brain hemispheres and stimulation sites in the 2 animals. - - -, the position of the recording chamber; ●, the penetration sites. The genu of the arcuate sulcus and the midline are indicated. The horizontal line runs tangentially to the genu of the arcuate sulcus.

phase (VOR phase) starts when Es becomes stationary and ends when the head stops moving. During this phase the Hs is still moving and the Eh starts rolling back in the head keeping Es at the same position. The VOR phase is a typical feature of normal gaze shifts and it is due to activation of the vestibuloocular reflex (VOR) that stabilizes Es during head motion.

Most comparable previous studies have focused on the gaze shift phase of such movements. However, because the VOR phase is more important for perception and motor control, we examine both phases here. Figure 2, *right*, shows the correspondent velocity profiles for the signals in the *left*. Es velocities reached higher peak values than the Hs and Eh velocities suggesting that the displacement of the Es is due to the additive interaction of Hs and Eh movements.

Stimulus-evoked movement latencies

Movements latencies were defined as the time from stimulus onset to movement initiation. Figure 3*A* shows histograms of the distributions of the Es (■) and Hs (□) average latencies for the 55 included sites. ▨ represents the overlapping between the two distributions. The latencies for Es and Eh movements were indistinguishable, so only the former is represented in the figures. The mean latency for Es (mean = 39 ms, ▶) was significantly smaller than the mean latency for Hs (mean = 55 ms, ▷). Within sites, the Hs latency was in all cases longer than the Es and Eh latency ($P < 0.05$, paired *t*-test). Figure 3*B* plots latencies (ordinate) as a function of gaze amplitude. This last measurement was obtained by computing the Es characteristic vector (CV) for each site, which represent the average movement that would be elicited when stimulating the site with the animal looking straight ahead (see METHODS). Es latencies from sites corresponding to *M1* are represented by ■ and the ones corresponding to *M2* by the ●. Hs latencies from sites corresponding to *M1* are represented by □ and those corresponding to *M2* by ○. For both animals, latencies are clearly shorter for the Es relative to the Hs; neither of the two groups of latencies varied as a function of gaze amplitude.

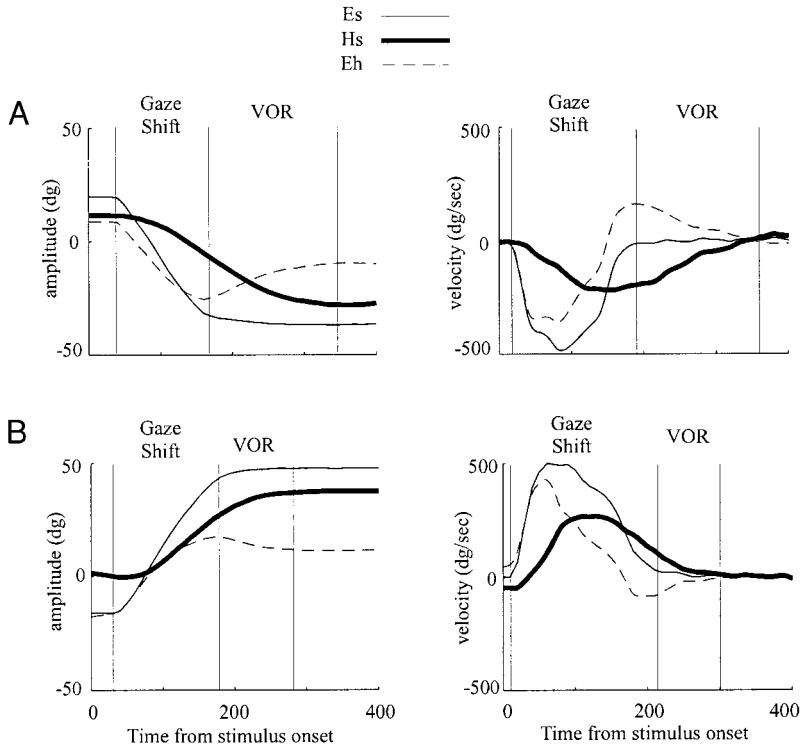

FIG. 2. Examples of stimulation-evoked movements. *Left*: plots of position signals (ordinate) as a function of time from stimulus onset (abscissa) recorded during the stimulation of 1 site in the right (*A*) and another in the left (*B*) supplementary eye field (SEF) of *M1*. *Right*: the correspondent velocity signals. The thin solid line represents eye-in-space (Es), the thick solid line head-in-space (Hs), and the dashed line eye-in-head (Eh). The vertical lines indicate the beginning and end of the gaze shift and vestibuloocular (VOR) phases.

Amplitude and directions of the evoked movements

To determine the average amplitude of the Es, Hs, and Eh movements across different sites, we first obtained two-dimensional trajectories of all the stimulation-evoked movements for each one of the sites. Figure 4 shows examples of trajectories evoked by stimulating one site in the left SEF (*left*) and another site on the right SEF (*right*) of M1. From *top* to *bottom*, *top* shows behind views of Es; *middle top* shows views of Eh, and *bottom middle* shows Hs trajectories during the gaze-shift phase of the movements. *Bottom* shows similar views of Hs trajectories but during both the gaze shifts and the VOR phase of the movements. The lines represent the trajectories and the circles their endpoints. In both cases Es, Hs, and Eh movements in the same direction but contralateral to the stimulated site were consistently evoked. For the site represented on the *left*, there is a clear difference in the amplitude of the Hs movements depending on whether the VOR phase (*bottom*) is included as part of the movement.

So far, the previous examples suggest that both the Hs and Eh contribute to the Es movements. To corroborate this, we quantified the amplitude of the movements across the different sites by computing the movements characteristic vector (CV, see METHODS). Figure 5*A* shows gaze trajectories evoked by stimulating one site on the right SEF in *animal M2* and their CV (black arrow). The lines represent the trajectories and the circles their final positions. The CV is pointing downward and to the left, like many of the individual trajectories. Note that individual trajectories could be larger or smaller that the CV, the latter represents the population.

Figure 5*B* shows a behind view of the spatial distribution of the CV for Es at the end of the gaze shift period. The circles represents data from *animal M1* and the squares from *M2;* they both represent the tip of the correspondent CVs. They were homogeneously distributed at both sides of the vertical merid-

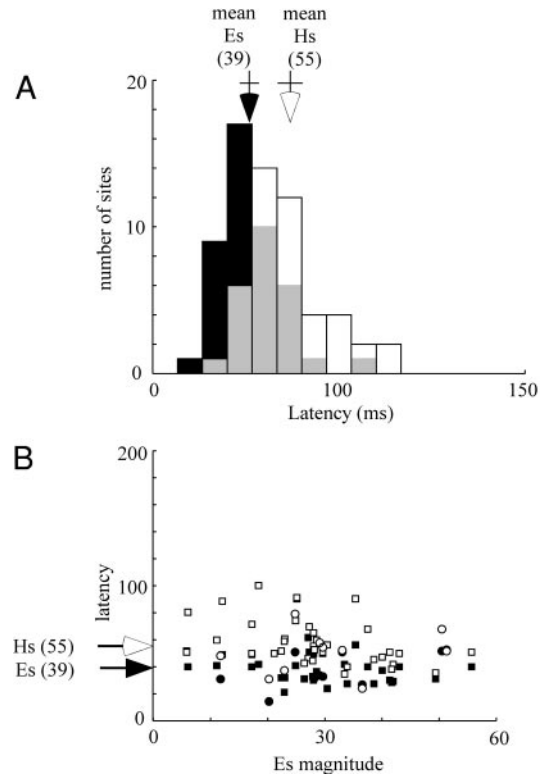

FIG. 3. Stimulation-evoked movements latencies. *A*: distribution of the Es (■) and Hs (□) evoked movement latencies for the 55 stimulation sites included in the analysis. The abscissa represents the latency in milliseconds and the ordinate the number of sites. ▨ the region of overlapping between the 2 distributions. Mean latencies are indicated (↓). The horizontal lines intersecting the arrows span the 95% confidence intervals for the mean. *B*: Es and Hs stimulation-evoked movements latencies (ordinate) as a function of gaze amplitude (abscissa). ■ and □, latencies for *animal M1;* ● and ○, latencies for *animal M2*. ■ and ●, Eh latencies; □ and ○, Hs latencies. Mean latencies are indicated.

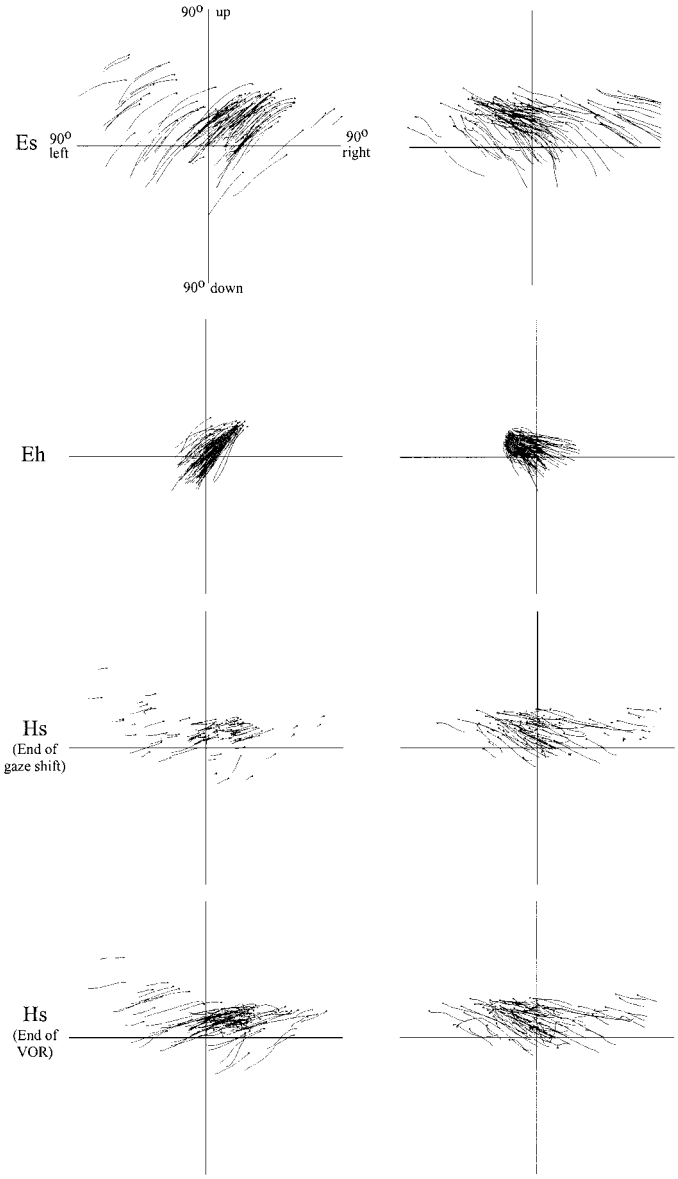

FIG. 4. Examples of stimulation-evoked movement trajectories. Behind view of trajectories evoked by stimulating 1 site in the left SEF of *M1* (*left*) and another in the right SEF of *M2* (*right*). The abscissa represents the horizontal meridian and the ordinate the vertical. The lines represent the trajectories, their free extreme represents the initial position and the circles represent the final position at the end of the gaze shift phase. *Top*: Es data; *middle top*: Eh data; *middle bottom*: Hs data. *Bottom*: Hs trajectories ending at the end of the VOR phase.

ian. Without exception, the sites in which CV are pointing to the right were left SEF sites and the sites with CV pointing to the left were right SEF sites. This rule corroborates the results of previous stimulation studies (Schlag and Schlag-Rey 1987). Interestingly we did not obtain CVs pointing in directions close to the vertical meridian. It is unlikely we missed sites encoding in those directions because we explored a substantial portion of the SEF.

Figure 5 shows the distribution of the Hs CVs for movements that finished at the end of the gaze shift phase (*C*) and for movements that finished at the end of the VOR phase (*E*). By inspection of these graphs, it can be noticed that the Hs CV amplitudes are larger at the end of the VOR relative to the end of the gaze shift because during the VOR phase the head continues moving until reaching its final position. The distributions of the Eh CV at the end of the gaze shift phase (*D*) and at the end of the VOR (*F*) are also shown. In this case, the amplitudes of the CVs are larger at the end of the gaze shift compared with the end of the VOR evidently because when the head moves during the VOR phase the Eh has rolled back to keep gaze stationary. Consistently with this, the CVs for gaze did not change during the VOR phase (not shown).

Figure 6 shows histograms of the distributions of the CVs amplitudes for Es (*A*), Hs (*B*), and Eh (*C*) at the end of the gaze shift (*top*) and at the end of the VOR (*bottom*). The small vertical lines at the top of each graph indicate the mean and the horizontal lines span the 95% confidence interval for the mean. Es CVs amplitudes ranged from 5 to 55°, although individual movements were much more variable (from 2 to 90°) across sites. The mean Es CVs amplitude was very similar at the end of the two periods (mean = 27° at the end of the gaze shift and mean = 29° at the end of the VOR, $P > 0.05$, paired *t*-test). For the Hs, the mean CV amplitude at the end of the gaze shift (*B*, mean = 11°) was significantly smaller than the mean at the end of the VOR (*E*, mean = 21°, $P < 0.05$, paired *t*-test). For the Es, the relationship is inverted, the mean CV amplitude was bigger at the end of the gaze shift (*C*, mean = 16°) than at the end of the VOR (*F*, mean = 10°, $P < 0.05$, paired *t*-test). In all cases, the mean CV amplitude were significantly different from zero ($P < 0.0001$, *z* test), demonstrating that both the head and eye systematically moved when stimulating the SEF. For the remainder of the results, we compared these movements to natural gaze shifts to see if they follow the same kinematics rules.

Comparison between stimulus-evoked movements and natural gaze shifts

We have previously noticed that the stimulation evoked movements seem to have a similar profile as natural gaze shifts. However, to prove that this is the case, a more rigorous analysis is needed. To perform such an analysis, we recorded a sample of natural gaze shifts made by the animals during the same recording sessions as when the stimulations were delivered. Figure 7 shows example of records from stimulation-evoked movements (*A* and *C*) and natural movements (*B* and *D*). *Left* horizontal position signals for Es (thin solid line) and its two components, Hs (thick solid line) and Eh (dashed line). The velocity signals that correspond to the position traces shown on the *left* are shown on the *right.* By casual inspection of these signals, either position or velocity, it is hard to differentiate between the stimulation-evoked and natural movements. The gaze shift and VOR phases are present in all the movements, and the signals' profiles appear very similar.

To quantify these similarities, we compared three different aspects of the movements: the velocity-amplitude movements profile, the eye-head contribution to the movements amplitude, and the constraints governing the three-dimensional movements kinematics. These comparisons were made between two samples of >800 stimulation evoked movements and approximately the same amount of natural gaze shifts in each animal. Because the Es initial and final positions were similar between the two samples, all movements were classified according to

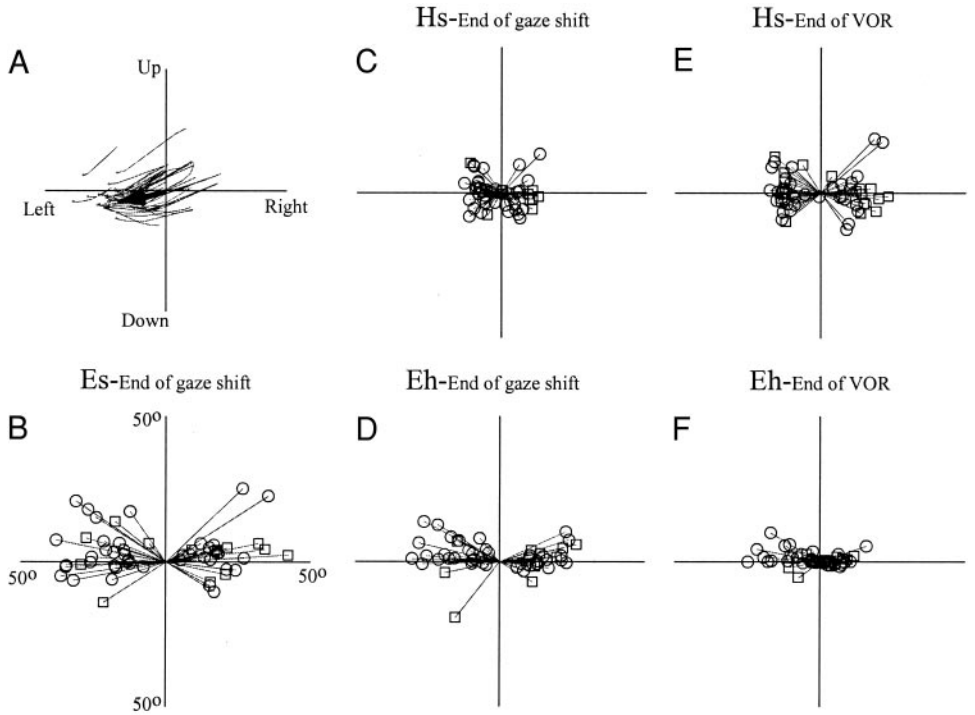

FIG. 5. Spatial distributions of the characteristic vector (CV). *A*: behind view of the trajectories evoked by stimulating 1 site in the right SEF of *M2* and its CV (dark arrow). The symbols are the same as the ones used in Fig. 4. *B*: behind view of the spatial distribution of the Es CVs across sites. The tip of the CVs from *M1* are represented by the circles and for *M2* by the squares. *C* and *D*: Hs and Eh CV distributions at the end of the gaze shift. *E* and *F*: Hs and Eh CV distributions at the end of the VOR.

their amplitude and then pooled within each sample for quantitative comparisons of kinematics between the two samples.

VELOCITY-AMPLITUDE PROFILES. For natural gaze shifts in the head-free macaque, the peak velocities of the Es, Hs, and Eh vary stereotypically as a function of gaze amplitude. We assessed whether the stimulation-evoked movements showed a similar variation by comparing the curves relating these two variables between the samples of stimulation-evoked and natural gaze shifts.

First, for each movement, its peak angular velocity as well as its amplitude were obtained. Then, movements were grouped in different bins according to their amplitude, and the average peak velocity for that bin was computed. Bins were 10° in amplitude for all cases. As a result, curves relating the average peak velocity of Es, Hs, and Eh and the movements amplitude, for each sample, were obtained. Figure 8 plots the peak velocities (ordinate) as a function of movement amplitude (abscissa) for Es (*top*), Hs (*middle*), and Eh (*bottom*). In all the graphs, the stimulation-evoked movements are represented by ■ and the natural gaze shifts by ○. *Left* displays data from *animal M1*, whereas data from *M2* are on the *right*. For Es, the peak velocity grew approximately linearly as a function of gaze amplitude until reaching ~40° where it saturates. For the Hs, the peak velocity grows approximately linearly as a function of the head movement amplitude. Finally, for the Eh the peak velocity grew approximately linearly with the movement amplitude until reaching 40–50°, close to the oculomotor limit for most movements originating near the center of the oculomotor range.

We compared the two data sets (stimulation-evoked vs. natural) in each one of the three cases (Es, Hs, and Eh) using a single-factor repeated-measures ANOVA test with gaze shift type (stimulation-evoked or natural) as within-subject factor. We did not find differences between the two types of move-

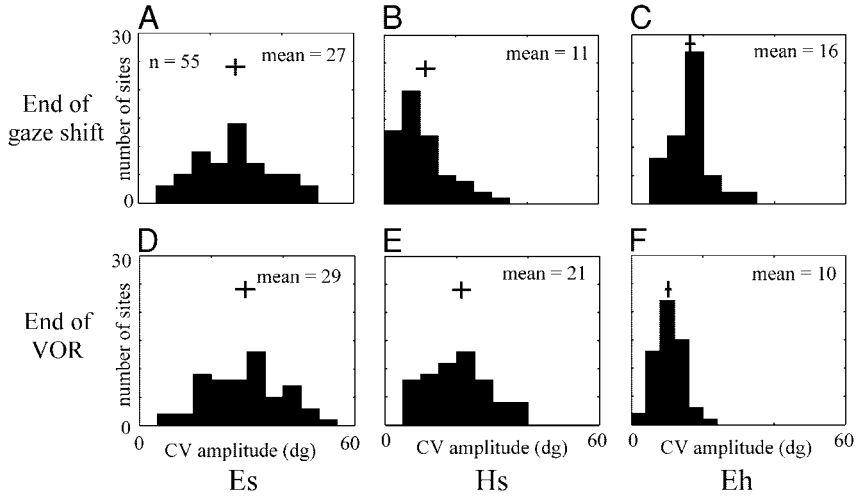

FIG. 6. Distribution of the CV amplitudes. In each histogram the abscissa represents the amplitude of the CV and the ordinate the number of sites. *Left*: Es (*A* and *D*); *middle*: Hs (*B* and *E*); *right*: Eh (*C* and *F*) data. *Top*: the CV were computed from movements ending at the end of the gaze shift phase. *Bottom*: the CV were computed from movements ending at the end of the VOR phase. The small vertical lines represent the mean of the distributions and the horizontal lines span their 95% confidence intervals.

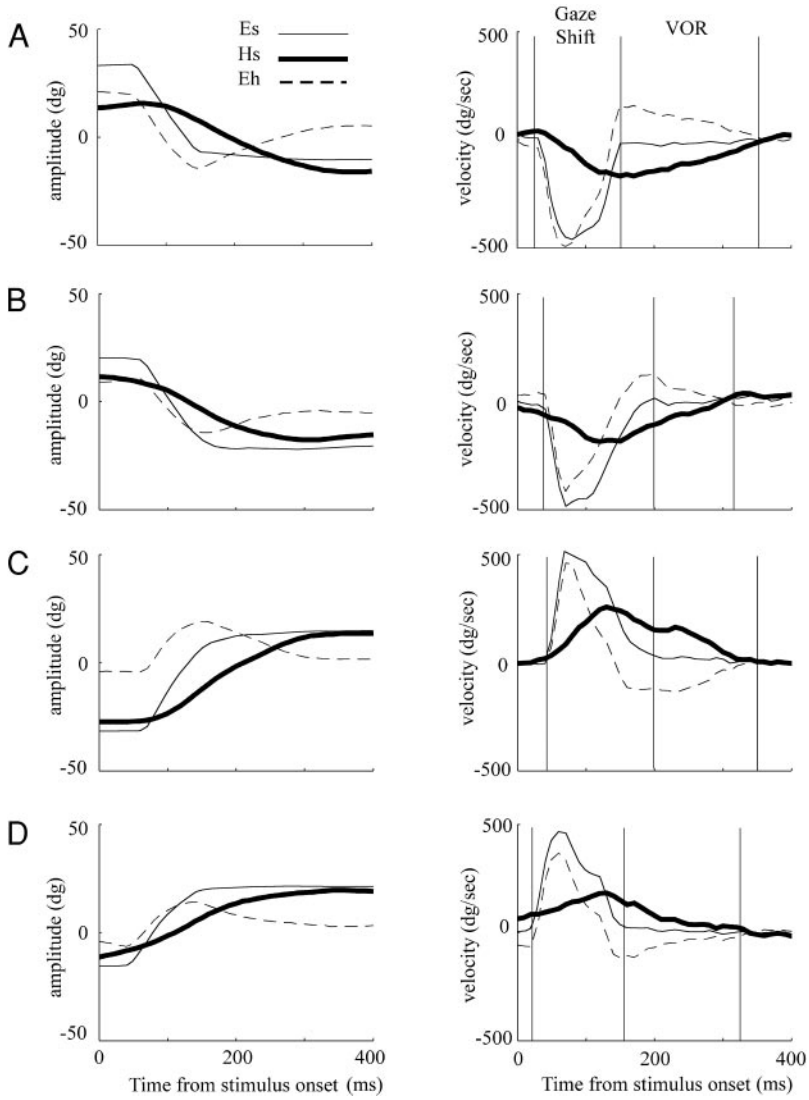

FIG. 7. Examples of stimulation-evoked movements and natural gaze shifts. The symbols are the same as the ones used in Fig. 2. *Left*: horizontal position signals; *right*: velocity profiles for the Es (thin solid line), Hs (thick solid line) and Eh (dashed line). *A* and *C*: stimulation-evoked movements from 2 different sites on the right (*A*) and left (*C*) SEF of *M1*. *B* and *D*: natural gaze shifts made by the same animal. The beginning and end of the gaze shift and VOR phases are indicated (*right*).

ment in any of the three cases (Es, Hs, and Eh) and in any of the animals ($P > 0.05$ in all cases, ANOVA test for within-subject effects). These results suggest that in this aspect of the movement kinematics the stimulation-evoked movements and natural gaze shifts were essentially the same.

EYE-HEAD CONTRIBUTION. Another aspect of movements kinematics that characterizes natural gaze shifts is the relationship between the relative contributions of the Hs and Eh to the movements amplitude and the amplitude of the gaze shift. Thus we assessed whether the stimulation-evoked movements were similar to natural gaze shifts in this aspect. For each movement, we determined the amplitude of the Es, Hs, and Eh trajectories. Then, the two samples (stimulation-evoked and natural gaze shifts) were segregated, and curves relating Hs and Eh movements amplitude with gaze amplitude were obtained for each sample. For more clarity, the data were grouped in bins of 10° according to the gaze shift amplitudes. Figure 9, *top*, shows the Hs contribution to the movements (ordinate) as a function of the Es movements' amplitude (abscissa) for the stimulation-evoked (■) and the natural gaze shifts (○). The Hs contribution grew approximately linearly as a function of the Es movement amplitude. On the other hand, the Eh contribution (*bottom*) grew monotonously as a function of gaze amplitude until reaching ~40°, where it saturates.

To compare the relative contribution of the Hs and Eh to the movements amplitude between the stimulation-evoked and natural gaze shifts, a similar procedure as the one used for the amplitude-peak velocity relationship was followed. A repeated-measures ANOVA test with movement type (stimulation-evoked vs. natural) as within-subject factor revealed that in both animals the relative contribution of the Hs and Eh to both movement types was the same ($P > 0.05$ in all cases, ANOVA test for within-subject effects). This result suggests that in this aspect of the movements kinematics the stimulation-evoked movements and natural gaze shifts were essentially the same.

For the stimulation-evoked movements, we have demonstrated that the head contribution increases when including the VOR phase as part of the movement (see Fig. 5). Here we wished to see if this increase was similar for the samples of stimulation-evoked movements and natural gaze shifts. We computed a contribution index (Hs movement amplitude – Eh movement amplitude)/(Hs movement amplitude + Eh movement amplitude) for each movement at the end of the gaze shifts and at the end of the VOR. Index values lower than zero

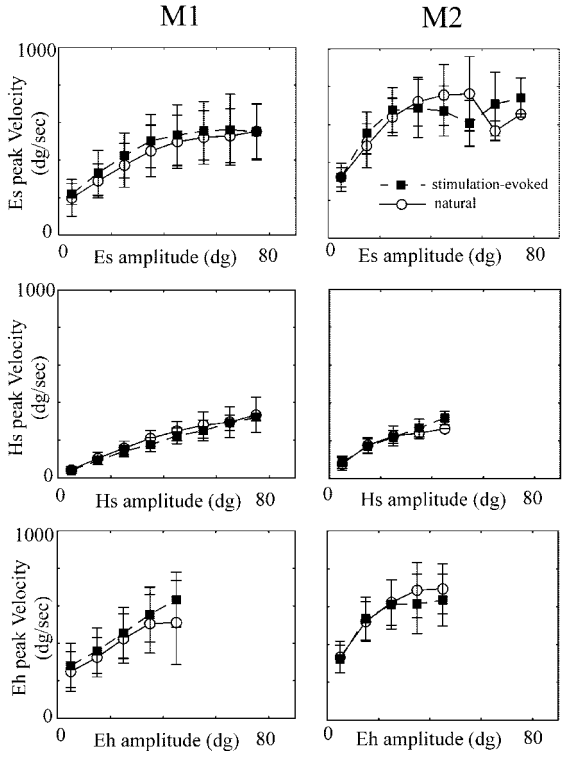

FIG. 8. Amplitude-velocity relationships of the movements. The panels show the averaged peak velocities (ordinate) of Es (*top*), Hs (*middle*), and Eh (*bottom*) as a function of the movements amplitude (abscissa). ■, data from stimulation-evoked movements; □, data from natural gaze shifts. The error bars represent SDs. *Left*: data from *animal M1; right*: data from *M2*.

indicate that the Hs contribute less than the Eh; an index value of zero indicates that the contributions are equal; and a positive index value indicates that the Hs contribute more than the Eh. For each animal, the movements index values were first divided into two groups (stimulation-evoked and natural gaze shifts) and then they were pooled within each group across the different sites (45 in *M1* and 10 in *M2*). Finally, each one of these two data sets was grouped in bins of 10° according to the

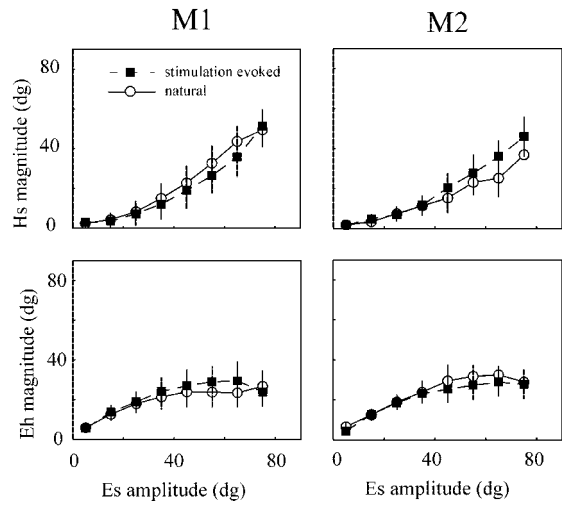

FIG. 9. Relative contributions of the Hs and Eh to the movements. Contribution of the Hs (ordinate in the *top*) and Eh (ordinate in the *bottom*) to the movements as a function of Es movements' amplitude (abscissa) for natural gaze shifts and stimulation-evoked movements. Symbols are the same as in Fig. 8. *Left*: data from *animal M1; right*: data from *M2*.

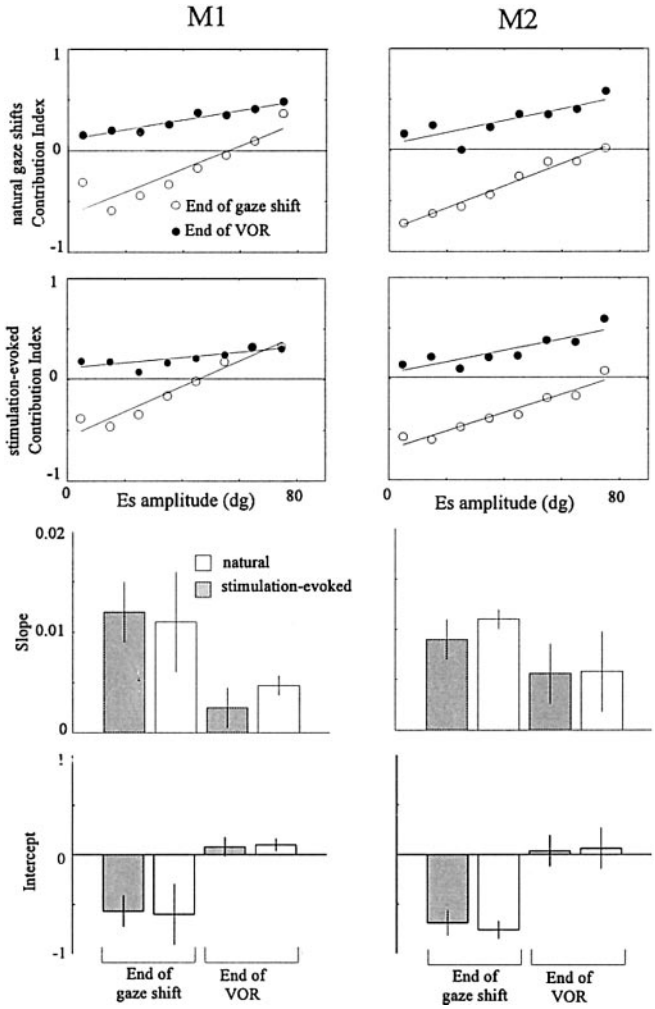

FIG. 10. Relative contribution of the Hs and Eh during the different movement phases. *Top* and *middle top*: the indices (Hs movement amplitude – Eh movement amplitude)/(Hs movement amplitude + Eh movement amplitude) in the ordinate as a function of Es movements amplitude (abscissa) at the end of the gaze shift (○) and at the end of the VOR (●). —, the best linear regression models fitted through the data. *Top*: data from natural gaze shifts; *middle top*: data from stimulation-evoked movements. *Left*: data from *M1; right*: data from *M2*. *Middle bottom, bottom*: the bar graphs represent the slopes of the lines shown in *top* and *middle top* and the intercepts of the same lines, respectively. The error bars represents the 95% confidence intervals.

Es movements amplitude and a mean index value for each bin was obtained.

The *top two rows* of Fig. 10 show the mean index values (ordinate) as a function of the Es movements amplitude (abscissa) for both animals (*M1* and *M2*). The *top* displays data obtained from natural gaze shifts and the *middle top* data for stimulation-evoked movements. The ○ represent the mean contribution indices for each bin at the end of the gaze shift period and the ● represent the indices at the end of the VOR period. The four data sets in the two animals have been fitted with linear regression models and the lines representing the best fit through the data are displayed. For each line, the slope, the intercept, and their correspondent 95% confidence intervals were obtained.

For indices at the end of the gaze shift, the slopes of all the lines are positive, indicating that in all cases the head contribution increases with the length of the movements. However,

for indices at the end of the VOR period, the slopes are significantly smaller. This is true for both, the stimulation-evoked and the natural movements. This result is better illustrated in Fig. 10, *middle bottom.* The bars represent the slopes of the lines and the error bars their 95% confidence intervals. For *M1*, there was a significant decrease in slope at the end of the VOR phase for both, stimulation-evoked and natural movements (the 95% confidence intervals for the slopes at the end of gaze and at the end of the VOR do not overlap; Fig. 10, *left, middle bottom*). *M2* showed the same trend although the decrease in slope for the stimulation-evoked movements was not significant (the 95% confidence intervals at the end of gaze and at the end of the VOR overlap; Fig. 10, *right, middle bottom*).

In addition, we compared the intercept of the lines at the end of the two periods. This is illustrated in the graphs shown in Fig. 10, *bottom.* At the end of the gaze shift, the intercepts were in all cases lower than −0.55, meaning that for the smallest movements the head contribution was ≥70% smaller than the eye contribution. This was true for the two movement populations in both animals. However, at the end of the VOR, the intercept of the lines became significantly higher as illustrated by the absence of overlap between the 95% confidence intervals of such intercepts with those of the intercepts at the end of the gaze shift (see Fig. 10, *bottom*).

When comparing the slopes and intercepts of the stimulation-evoked movements versus the ones of natural gaze shifts within the same period, there was a considerable degree of overlapping between the 95% confidence intervals in all cases (end of gaze and end of the VOR) and for the two animals, suggesting that they were not significantly different. To further corroborate this last result, we compared the mean index values between the two kinds of movement and at the end of the two phases. For this purpose, we pooled the data from both animals and performed a repeated-measures ANOVA test with movement type as within subject factor. The comparison revealed no differences between the indices for the two kinds of movements ($P > 0.05$, ANOVA test for within-subject effects). This holds for the two cases, at the end of the gaze shift and at the end of the VOR.

One additional detail in the same Fig. 10 is that at the end of the gaze shift period the contribution of the Eh is larger than the one of the Hs except for movements larger than or equal to 60–70°. This is quite different from the kinematics at the end of the VOR period where the Hs contribution is always larger than the Eh contribution. This was true for both the stimulation-evoked movements and natural gaze shifts in both animals.

In summary, from the previous analysis, we can conclude first that the stimulation-evoked movement and natural gaze shifts were essentially the same with regard to the relative contribution of the eyes and the head to the movements amplitude. This result held for both the two movement phases, the gaze shift and the VOR phase. Second, at the end of the VOR, the relative contribution of the head to the movement increased even for small movements. This was very likely due to the completion of the final phase of head motion that tends to align the head with the gaze pointing direction.

3-D KINEMATICS. During natural fixations, the eyes and the head approximate Donders' law (Donders 1848), which states that for any one two-dimensional (vertical and horizontal) gaze pointing direction, there is a unique and constant amount of torsional rotation. These 3-D constraints have been shown to be obeyed most closely during fixations at the end of the VOR phase of natural gaze shifts in monkeys (Crawford et al. 1991, 1999) and at the end of the similar phase of gaze shifts evoked by stimulating the SC (Klier et al. 2002b). Moreover, it has been shown that this can only occur if the eyes and head are very precisely coordinated. Here we similarly assessed whether the same constraints are obeyed at the end of the movements evoked by stimulating the SEF.

First we computed 3-D position quaternions for the Es, Hs, and Eh during natural fixations and fitted 3-D surfaces to them (see METHODS). Figure 11, *left*, shows data from one example experiment in *animal M1*. The graphs display the horizontal components (ordinate) of the axis of rotations (quaternions converted to angles) for the Es (*top*), Hs (*middle*), and Eh (*bottom*) as a function of the torsional components (abscissa) plotted in right-hand rule coordinates. For example, a data

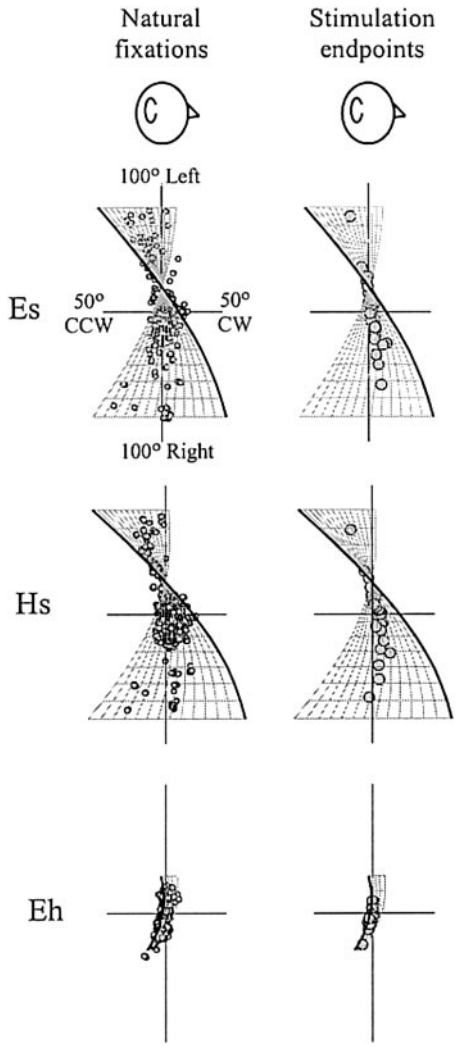

FIG. 11. 3-D analysis for 1 stimulation site. Scatter plots of the torsional (abscissa) and horizontal (ordinate) components of Es (*top*), Hs (*middle*), and Eh (*bottom*) position quaternions converted to angles of rotation in right-hand rule coordinates. *Left*: natural fixations; *right*: stimulation endpoints. Three-dimensional surfaces fitted to the data points are represented, the forward vertical edges of the surfaces has been highlighted (black thick line) to facilitate visual interpretation of these 3-dimensional plots.

point falling in the left upper quadrant represents a counterclockwise and leftward movement. The planes represent the Donders' surfaces (2-dimensional range given by the best polynomial fit through the data). Observe that the forward vertical edge of the surfaces has been highlighted (black thick line) to facilitate visual interpretation of these three-dimensional plots.

For oblique (horizontal-vertical) positions far away from the center, the Es and Hs surfaces show larger deviations from the ordinate than the Eh surface, corroborating that for the Es and Hs Donders' law is obeyed but not Listing's law (Crawford et al. 1999). In contrast, the Eh falls within a flat surface similar to the Listing's plane observed with the head fixed (Tweed and Vilis 1990).

Figure 11, *right*, displays the same surfaces as on the *left* (fit to the behavioral data), but in this case, the data at the end of the stimulation-evoked movements are over plotted on the surfaces. These stimulation data seems to adhere quite well to the surfaces, suggesting that at the end of the stimulation-evoked movements Donders' and Listing's law are also obeyed.

However, the space fixed coordinate system we have used to plot the data in Fig. 11 does not allow to correctly appreciate the relatively tight 3-D control of Es, Hs, and Eh positions relative to the curved and twisted Donders' surfaces. This is better seen by plotting the stimulation-evoked data in a new coordinate system (Donders' coordinates) in which the vertical and horizontal axis are aligned with the Donders' surface and the torsional axis remains fixed in space. Figure 12 displays stimulation endpoints for the Es (*top*), Hs (*middle top*), and Eh (*middle bottom*) for two examples, one from *M1* (*left*) and another from *M2* (*right*) in Donders' coordinates. Observe that in this new coordinate system the abscissa represents the deviation of the data from the surface and the ordinate the surface. In all cases, the data are equally and closely distributed at both sides of the ordinate, reflecting that they adhere well to their correspondent surfaces. In both examples, there is more spread along the horizontal axis for the Es, followed by the Hs and much less for the Eh reflecting a tighter control of the torsional component of the movement for the Eh relative to the Hs and Es.

To quantify this spread, we determined the mean deviation of the data from the point of zero torsion, in this case from the ordinate. This measurement, known as torsional SD, has been already used in previous studies of 3-D gaze kinematics (Crawford et al. 1999; Glenn and Vilis 1992; Klier et al. 2002b; Radau et al. 1994). Figure 12, *bottom*, has bar graphs that display the torsional SDs of the stimulation end points for the Es, Hs, and Eh. The first example, from *animal M1*, showed average torsional SDs of 4, 3.1, and 1.5° for the Es, Hs, and Eh, respectively. The second example, from *animal M2*, showed somehow higher torsional SDs, 9.4, 7.1, and 1.8° for the Es, Hs, and Eh respectively. This is equivalent to less consistent torsional control of the head in *M2*. In both examples, the Es and Hs showed higher torsional SDs than the Eh, a result similar to the one reported for natural gaze shifts in the head-free macaque (Crawford et al. 1999). This analysis was done for each stimulation site. As a control the torsional SD of the natural fixation data were also calculated.

Figure 13 summarizes the results of this analysis for the two animals. It shows the average torsional SDs across sites for the

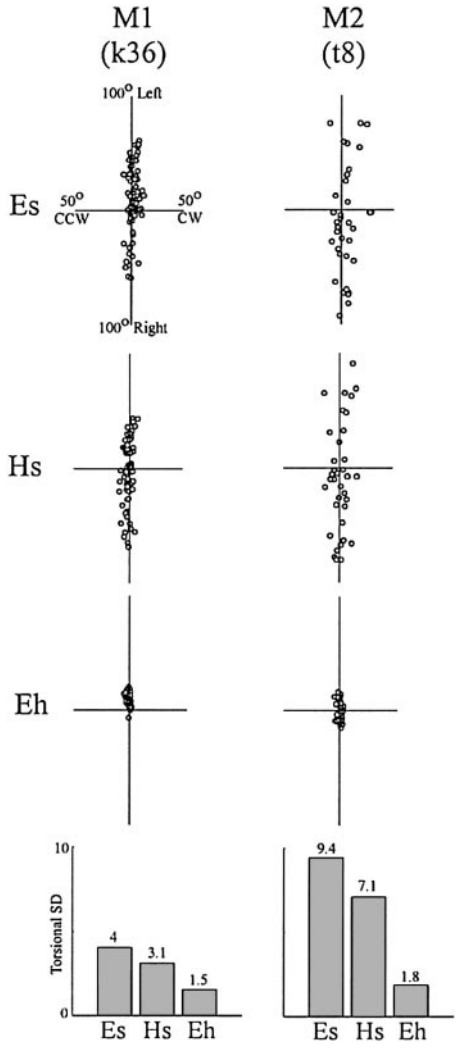

FIG. 12. Stimulation end points in Donders' coordinates. Scatter plots of the stimulation end points quaternions torsional components (abscissa) against the horizontal components (ordinate) in Donders' coordinates. The symbols are the same as in Fig. 11. *Top*: Es; *middle top*: Hs; *middle bottom*: Eh data. *Left*: data are from 1 example in *animal M1; right*: data from another example in *animal M2*. *Bottom*: bar graphs display the average torsional SDs for each component (Es, Hs, and Eh).

natural fixations (*top*) and for the stimulation-evoked movements (*bottom*). In each case, the Es and Hs average torsional SDs were significantly larger than the one for the Eh ($P < 0.05$, paired *t*-test). More important, for the two animals, both datasets (natural fixations and stimulation-evoked endpoints) follow the same pattern. No significant differences were found between them ($P > 0.05$, paired *t*-test). In summary, our analysis has shown that at the end of the stimulation-evoked movements the same 3-D constraints as during natural fixations are obeyed corroborating that the evoked movements were indistinguishable from natural gaze shifts.

DISCUSSION

The present study was aimed to determine the nature of the motor output of the SEF. We found that in 55 sites electrical stimulation with the parameters we have employed (see METHODS) evoked Es movements with regular latencies. Such move-

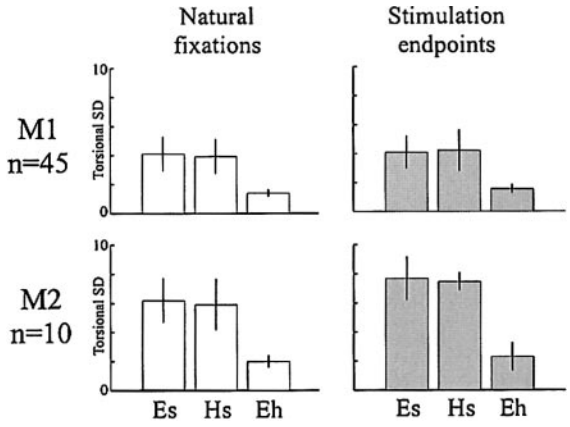

FIG. 13. Average torsional SDs. Average torsional SDs during natural fixations (*left*) and stimulation end points (*right*). The abscissa displays Es and its 2 components (Hs and Eh) and the ordinate the average torsional SD in degrees. *Top*: data from *M1; bottom*: data from *M2*. The error bars represents SDs.

ments were a combination of Hs and Eh rotations. Their two- and three-dimensional kinematics (velocity-amplitude relationship, relative contributions of the eyes and head to the movements, and Donders' law) were indistinguishable from the one of natural gaze shifts. These results demonstrate that the motor output of the SEF is a gaze command composed of coordinated Hs and Eh movements. The relative contribution of these components to gaze as well as other kinematics aspects of eye-head coordination during gaze shifts are very likely implemented in structures located downstream from the SEF.

Stimulation studies in the SEF

We systematically stimulated a considerable number of SEF sites in two head-free animals and found that head and eye movements were consistently evoked. One possible difference between ours and previous stimulation studies in the SEF (Schlag and Schlag-Rey 1987), where they reported a low rate of success in evoking head movements, is that these authors performed a substantial number of stimulations when the animals had their head fixed. Their animals could have adopted new eye-head coordination strategies during the experimental sessions (i.e., decreasing the head contribution and maximizing the eye contribution to gaze). If such strategies are implemented downstream from the SEF and they are active when the stimulation was delivered, it will likely evoke the same learned pattern of behavior. This hypothesis is supported by experimental data showing that monkeys change their eye-head coordination strategies depending on new conditions (Ceylan et al. 2000; Crawford and Guitton 1997), and at least part of these learned strategies can be preserved during stimulation of the SC (Constantin et al. 2000). In our study, we avoided this potential problem by minimizing the amount of time that the animals were with their heads restrained during the training and recording sessions. Therefore the eye-head coordination strategies were relatively intact when delivering the stimulation.

Another possibility that could explain the differences between the studies is that different animals could have different eye-head coordination strategies during natural gaze shifts. This phenomenon has been already described in humans, different individuals can be classified as head movers and non-head movers when performing the same visuomotor tasks (Fuller 1992, 1996; Stahl 2001).

Finally, it could also simply be because their small sample size, whereas we thorough explored the SEF with the head free.

Furthermore, we demonstrated that the kinematics of the stimulation-evoked movements were indistinguishable from the one of natural gaze shifts. The stereotyped pattern of relationships between peak velocity and movement amplitude as well as head/eye movement amplitude and movement amplitude followed by natural gaze shifts was clearly present in the evoked movements. The 3-D constraints described from natural gaze shifts was also obeyed by the stimulation evoked movements demonstrating that the precisely tuned mechanisms implementing eye-head coordination during natural gaze shifts are engaged by SEF stimulation. These results suggest that the movements generated by stimulating the SEF were coordinated gaze shifts. Therefore we conclude that the motor output of the area is gaze.

Stimulation studies in other brain areas

In comparison, the report of Tu and Keating (2000) demonstrated that electrical stimulation of the FEF evokes combined movements of the eyes and the head that were qualitatively similar to natural gaze shifts. These authors suggested that the FEF encodes gaze. However, they did not systematically compare the kinematics of the evoked-movements and natural gaze shifts; therefore one cannot discard that the FEF is involved in other aspects of motor control rather than gaze coding. Interestingly, the relationship between the movements mean latency for the Eh (47 ms) and the Hs (58 ms) reported in the FEF is similar to the one we have found in the SEF (Eh latency = 39 ms, Hs latency = 55 ms). In both cases, the head latency was longer than the eyes latency by 10–15 ms. This suggests that a similar command can be sent from both areas to lower centers. This is supported by anatomical data showing that the FEF (Segraves 1992) and the SEF (Shook et al. 1990) directly project to oculomotor structures in the brain stem.

In the SC, it has been also reported that electrical stimulation evokes combined movements of the eyes and the head that obey the same kinematics rules as natural gaze shifts (Freedman et al. 1996; Klier et al. 2001). It has been proposed that the SC encodes gaze and that the implicit kinematics aspects of the movements are specified by structures located downstream. This finding supports our hypothesis that structures in the frontal cortex play an important role in visuomotor coding and are less concerned with specific aspects of eye-head coordination. Interestingly, although there is a striking similarity between the stimulation parameters (current intensities and duration) that seem to be optimal for evoking combined eye/head gaze shifts in the frontal cortex and the SC, there is a considerable gap between the latencies reported by Freedman and coworkers (1996) in the SC (~35 ms) and those we found in the SEF (~50 ms). This likely reflects first, that neurons within these areas (SEF, FEF, and SC), that encode gaze, are closely connected and probably share similar properties and, second, that an additional amount of processing takes place in the SEF before the gaze command is released toward the FEF, the SC, and brain stem structures.

But why such a redundancy of gaze generators in the brain?

One possibility is that the different areas play different roles in visuomotor transformations or other high level cognitive functions. For example, it has been reported that the SEF is involved in performing reference frame transformations (Olson and Gettner 1999; Olson and Tremblay 2000), attentional processing (Bon and Luchetti 1997), decision making (Coe et al. 2002), planning of eye movement sequences (Lu et al. 2002; Schlag 2002), and probably other related high-level functions. Our current results and literature suggest that desired two-dimensional gaze direction is the common default language used by the SEF and other higher brain centers to specify targets, whereas other more specific aspects of eye-head coordination are implemented downstream from these structures, probably in the brain stem.

If one can generalize about these results, then one might speculate that the cortex is concerned mainly with the explicit *goals* of movements (in this case gaze), leaving the details of coordination, inverse kinematics, and kinematics redundancy (Donders' law, etc.) for subcortical structures. This does not mean that other cortical areas, which we might have missed in our stimulations, could not encode torsion or various aspects of eye-head coordination. Indeed, one can voluntarily change patterns of eye-head coordination, generate torsional head movements, and even learn to generate a torsional saccade without a head movement (Balliet and Nakayama 1978), probably through direct cortical-brain stem connections that bypass the superior colliculus. Similarly, the cortex clearly controls multiples degrees of freedom in complex, learned arm movements (Gandolfo et al. 2000; Georgopoulos 2000; Kermadi et al. 1998; Li et al. 2001). For a simple example, the arm rotates torsionally (a violation of Donders' law of the arm) to grasp objects like a door knob (Marotta et al. 2002). However, the common element among each of these eye, head, and arm examples is that the extra degrees of freedom are now part of the explicit goal of the movements. In contrast, when the explicit goal is underspecified—as a gaze shift, or a pointing movement—it seems likely that the redundant degrees of freedom are controlled implicitly by rules implemented in subcortical structures (Klier et al. 2002b). This would explain why during both normal behavior and cortical stimulation the eye-head coordination system shows stereotypical, lawful kinematics relationships like Donders law, main sequence, etc. (Guitton 1992; Robinson and Fuchs 2001; Sparks et al. 2001, 2002).

In summary, our study has shown that the output of the SEF is a gaze command composed of coordinated movements of the eye and the head. The relative contributions of these two structures to gaze seems to be determined downstream from this area. A question that remains to be answered is *how* the SEF encodes this gaze signal, for example as a desired position or displacement, and in which reference frame.

The authors thank E. M. Klier and M. A. Smith for useful comments during the preparation of this manuscript and S. Sun and X. Yan for technical support.

This work was supported by Canadian Institute for Health Research Grants to J. D. Crawford, who also holds a Canada Research Chair. J. C. Martinez-Trujillo was supported by a Premier's Research Excellence Award held by J. D. Crawford.

REFERENCES

Balliet R and Nakayama K. Training of voluntary torsion. *Invest Ophthalmol Vis Sci* 17: 303–314, 1978.

Bon L and Lucchetti C. The dorsomedial frontal cortex of the macaque monkey: fixation and saccade-related activity. *Exp Brain Res* 89: 571–580, 1992.

Bon L and Lucchetti C. Attention-related neurons in the supplementary eye field of the macaque monkey. *Exp Brain Res* 113: 180–185, 1997.

Ceylan M, Henriques DY, Tweed DB, and Crawford JD. Task-dependent constraints in motor control: pinhole goggles make the head move like an eye. *J Neurosci* 20: 2719–2730, 2000.

Chen LL and Sparks DL. Supplementary eye field contribution to gaze shifts studied by electrical microstimulation in head-free monkeys. *Neural Control Move Abstr* D11, 2001.

Chen LL and Wise SP. Supplementary eye field contrasted with the frontal eye field during acquisition of conditional oculomotor associations. *J Neurophysiol* 73: 1122–1134, 1995a.

Chen LL and Wise SP. Neuronal activity in the supplementary eye field during acquisition of conditional oculomotor associations. *J Neurophysiol* 73: 1101–1121, 1995b.

Coe B, Tomihara K, Matsuzawa M, and Hikosaka O. Visual and anticipatory bias in three cortical eye fields of the monkey during an adaptive decision-making task. *J Neurosci* 22: 5081–5090, 2002.

Constantin AG, Wang H, Klier EM, and Crawford JD. Context dependent adaptation of eye-head coordination in gaze saccades evoked by superior colliculus stimulation. *Socr Neurosci Abstr* 26: 1992, 2000.

Crawford JD, Cadera W, and Vilis T. Generation of torsional and vertical eye position signals by the interstitial nucleus of Cajal. *Science* 252: 1551–1553, 1991.

Crawford JD, Ceylan MZ, Klier EM, and Guitton D. Three-dimensional eye-head coordination during gaze saccades in the primate. *J Neurophysiol* 81: 1760–1782, 1999.

Crawford JD and Guitton D. Primate head-free saccade generator implements a desired (post-VOR) eye position command by anticipating intended head motion. *J Neurophysiol* 78: 2811–2816, 1997.

Crawford JD and Vilis T. Axes of eye rotation and Listing's law during rotations of the head. *J Neurophysiol* 65: 407–423, 1991.

Donders FC. Beitrag sur Lehre von den Bewegungen des menschlichen Auges. *Holland Beitr Anat Physiol Wiss* 1: 105–145, 1848.

Ferman L, Collewijn H, and Van den Berg AV. A direct test of Listing's law. II. Human ocular torsion measured under dynamic conditions. *Vision Res* 27: 939–951, 1987a.

Ferman L, Collewijn H, and Van den Berg AV. A direct test of Listing's law. I. Human ocular torsion measured in static tertiary positions. *Vision Res* 27: 929–938, 1987b.

Freedman EG and Sparks DL. Eye-head coordination during head-unrestrained gaze shifts in rhesus monkeys. *J Neurophysiol* 77: 2328–2348, 1997.

Freedman EG, Stanford TR, and Sparks DL. Combined eye-head gaze shifts produced by electrical stimulation of the superior colliculus in rhesus monkeys. *J Neurophysiol* 76: 927–952, 1996.

Fuller JH. Head movement propensity. *Exp Brain Res* 92: 152–164, 1992.

Fuller JH. Comparison of horizontal head movements evoked by auditory and visual targets. *J Vestib Res* 6: 1–13, 1996.

Fujii N, Mushiake H, Tamai M, and Tanji J. Microstimulation of the supplementary eye field during saccade preparation. *Neuroreport* 6: 2565–2568, 1995.

Gandhi NJ and Sparks DL. Experimental control of eye and head positions prior to head unrestrained gaze shifts in monkey. *Vision Res* 41: 3243–3254, 2001.

Gandolfo F, Li C, Benda BJ, Schioppa CP, and Bizzi E. Cortical correlates of learning in monkeys adapting to a new dynamical environment. *Proc Natl Acad Sci USA* 97: 2259–2263, 2000.

Georgopoulos AP. Neural aspects of cognitive motor control. *Curr Opin Neurobiol* 10: 238–241, 2000.

Glenn B and Vilis T. Violations of Listing's law after large eye and head gaze shifts. *J Neurophysiol* 68: 309–318, 1992.

Guillaume A and Pelisson D. Gaze shifts evoked by electrical stimulation of the superior colliculus in the head-unrestrained cat. II. Effect of muscimol inactivation of the caudal fastigial nucleus. *Eur J Neurosci* 14: 1345–1359, 2001a.

Guillaume A and Pelisson D. Gaze shifts evoked by electrical stimulation of the superior colliculus in the head-unrestrained cat. I. Effect of the locus and of the parameters of stimulation. *Eur J Neurosci* 14: 1331–1344, 2001b.

Guitton D. Control of eye-head coordination during orienting gaze shifts. *Trends Neurosci* 15:174–179, 1992.

Helmholtz H. *Treatise of Physiological Optics* [English translation], translated by Southall JPC. Rochester, NY: Opt Soc Am, 1867.

Kermadi I, Liu Y, Tempini A, Calciati E, and Rouiller EM. Neuronal activity in the primate supplementary motor area and the primary motor cortex in relation to spatio-temporal bimanual coordination. *Somatosens Mot Res* 15: 287–308, 1998.

Klier EM, Wang H, Constantin AG, and Crawford JD. Midbrain control of three-dimensional head orientation. *Science* 295: 1314–1316, 2002a.

Klier EM, Wang H, and Crawford JD. The superior colliculus encodes gaze commands in retinal coordinates. *Nat Neurosci* 4: 627–632, 2001.

Klier EM, Wang H, and Crawford JD. Neural mechanisms of three-dimensional eye and head movements. *Ann NY Acad Sci* 956: 512–514, 2002b.

Levinsohn G. Uber die Bezihehungen der Grosshirnrinde beim Affen zu den Bewegungen des Auges. *Graefe Arch Ophthalmol* 71: 313–378, 1909.

Li CS, Padoa-Schioppa C, and Bizzi E. Neuronal correlates of motor performance and motor learning in the primary motor cortex of monkeys adapting to an external force field. *Neuron* 30: 593–607, 2001.

Lu X, Matsuzawa M, and Hikosaka O. A neural correlate of oculomotor sequences in supplementary eye field. *Neuron* 34: 317–325, 2002.

Marotta JJ, Medendorp WP, and Crawford JD. Contribution of the upper and lower arm to grasp orientation. *Soc Neurosci Abstr* 268.8, 2002.

Martinez-Trujillo JC, Klier EM, Wang H, and Crawford JD. Gaze shifts evoked by electrical stimulation of the SEF in the macaque monkey. *Soc Neurosci Abstr* 11.9, 2002.

Medendorp WO, Melis BJM, Gielen CCAM, and Van Gisbergen JAM. Off-centric rotation axis in natural head movements: implications for vestibular reafference and kinematics redundancy. *J Neurophysiol* 79: 2025–2039, 1998.

Missal M and Heinen SJ. Facilitation of smooth pursuit initiation by electrical stimulation in the supplementary eye fields. *J Neurophysiol* 86: 2413–2425, 2001.

Misslisch H, Tweed D, and Vilis T. Neural constraints on eye motion in human eye-head saccades. *J Neurophysiol* 79: 859–869, 1998.

Mitz AR and Godschalk M. Eye-movement representation in the frontal lobe of rhesus monkeys. *Neurosci Lett* 106: 157–162, 1989.

Olson CR and Gettner SN. Macaque SEF neurons encode object-centered directions of eye movements regardless of the visual attributes of instructional cues. *J Neurophysiol* 81: 2340–2346, 1999.

Olson CR and Tremblay L. Macaque supplementary eye field neurons encode object-centered locations relative to both continuous and discontinuous objects. *J Neurophysiol* 83: 2392–2411, 2000.

Pelisson D, Guitton D, and Munoz DP. Compensatory eye and head movements generated by the cat following stimulation-induced perturbations in gaze position. *Exp Brain Res* 78: 654–658, 1989.

Radau P, Tweed D, and Vilis T. Three dimensional eye, head and chest orientation after large gaze shifts and the underlying neural strategies. *J Neurophysiol* 72: 2840–2852, 1994.

Robinson FR and Fuchs AF. The role of the cerebellum in voluntary eye movements. *Annu Rev Neurosci* 24: 981–1004, 2001.

Roucoux A, Guitton D, and Crommelinck M. Stimulation of the superior colliculus in the alert cat. II. Eye and head movements evoked when the head is unrestrained. *Exp Brain Res* 39: 75–85, 1980.

Russo GS and Bruce CJ. Effect of eye position within the orbit on electrically elicited saccadic eye movements: a comparison of the macaque monkey's frontal and supplementary eye fields. *J Neurophysiol* 69: 800–818, 1993.

Russo GS and Bruce CJ. Neurons in the supplementary eye field of rhesus monkeys code visual targets and saccadic eye movements in an oculocentric coordinate system. *J Neurophysiol* 76: 825–848, 1996.

Russo GS and Bruce CJ. Supplementary eye field: representation of saccades and relationship between neural response fields and elicited eye movements. *J Neurophysiol* 84: 2605–2621, 2000.

Schall JD. Neuronal activity related to visually guided saccades in the frontal eye fields of rhesus monkeys: comparison with supplementary eye fields. *J Neurophysiol* 66: 559–579, 1991.

Schiller PH and Tehovnik EJ. Look and see: how the brain moves your eyes about. *Prog Brain Res* 134: 127–142, 2001.

Schlag JD. Neurons that program what to do and in what order. *Neuron* 34: 177–178, 2002.

Schlag J and Schlag-Rey M. Evidence for a supplementary eye field. *J Neurophysiol* 57: 179–200, 1987.

Segraves MA. Activity of monkey frontal eye field neurons projecting to oculomotor regions of the pons. *J Neurophysiol* 68: 1967–1985, 1992.

Shook BL, Schlag-Rey M, and Schlag J. Primate supplementary eye field. I. Comparative aspects of mesencephalic and pontine connections. *J Comp Neurol* 301: 618–642, 1990.

Sparks DL, Barton EJ, Gandhi NJ, and Nelson J. Studies of the role of the paramedian pontine reticular formation in the control of head-restrained and head-unrestrained gaze shifts. *Ann NY Acad Sci* 956: 85–98, 2002.

Sparks DL, Freedman DG, Chen LL, and Gandhi NJ. Cortical and subcortical contributions to coordinated eye and head movements. *Vision Res* 41: 3295–3305, 2001.

Stahl JS. Eye-head coordination and the variation of eye-movement accuracy with orbital eccentricity. *Exp Brain Res* 136: 200–210, 2001.

Tehovnik EJ, Lee K, and Schiller PH. Stimulation-evoked saccades from the dorsomedial frontal cortex of the rhesus monkey following lesions of the frontal eye fields and superior colliculus. *Exp Brain Res* 98: 179–190, 1994.

Tehovnik EJ, Slocum WM, Tolias AS, and Schiller PH. Saccades induced electrically from the dorsomedial frontal cortex: evidence for a head-centered representation. *Brain Res* 795: 287–291, 1998.

Tehovnik EJ, Slocum WM, and Schiller PH. Behavioural conditions affecting saccadic eye movements elicited electrically from the frontal lobes of primates. *Eur J Neurosci* 11: 2431–2443, 1999.

Theeuven M, Miller LE, and Gielen CCAM. Is the orientation of head and arm coupled during pointing movements? *J Mot Behav* 24: 242–250, 1993.

Tomlinson RD and Bahra PS. Combined eye-head gaze shifts in the primate. I. Metrics. *J Neurophysiol* 56: 1542–1557, 1986.

Tremblay L, Gettner SN, and Olson CR. Neurons with object-centered spatial selectivity in macaque SEF: do they represent locations or rules? *J Neurophysiol* 87: 333–350, 2002.

Tweed D. Three-dimensional model of the human eye-head saccadic system. *J Neurophysiol* 77: 654–666, 1997.

Tweed D, Cadera W, and Vilis T. Computing three-dimensional eye position quaternions and eye velocity from search coil signals. *Vision Res* 30: 97–110, 1990.

Tweed D and Vilis T. Geometric relations of eye positions and velocity vectors during saccades. *Vision Res* 30: 111–127, 1990.

Tu TA and Keating EG. Electrical stimulation of the frontal eye field in a monkey produces combined eye and head movements. *J Neurophysiol* 84: 1103–1106, 2000.